J. Ocean Univ. China (Oceanic and Coastal Sea Research)
DOI 10.1007/s11802-016-2690-9
ISSN 1672-5182, 2016 15 (1): 78-82
http://www.ouc.edu.cn/xbywb/
E-mail:xbywb@ouc.edu.cn

Experimental Study of Dissolved Oxygen Transport by Regular Waves Through a Perforated Breakwater

YIN Zegao[1), 2), *], YU Ning[2)], LIANG Bingchen[1), 2)], ZENG Jixiong[2)], and XIE Shaohua[2)]

1) *Shandong Province Key Laboratory of Ocean Engineering*, *Ocean University of China*, *Qingdao* 266100, *P. R. China*
2) *Engineering College*, *Ocean University of China*, *Qingdao* 266100, *P. R. China*

(Received June 14, 2014; revised December 31, 2014; accepted November 6, 2015)

Abstract The perforated breakwater is an environmentally friendly coastal structure, and dissolved oxygen concentration levels are an important index to denote water quality. In this paper, oxygen transport experiments with regular waves through a vertical perforated breakwater were conducted. The oxygen scavenger method was used to reduce the dissolved oxygen concentration of inner water body with the chemicals Na_2SO_3 and $CoCl_2$. The dissolved oxygen concentration and wave parameters of 36 experimental scenarios were measured with different perforated arrangements and wave conditions. It was found that the oxygen transfer coefficient through wave surface, K_1a_1, is much lower than the oxygen transport coefficient through the perforated breakwater, K_2a_2. If the effect of K_1a_1 is not considered, the dissolved oxygen concentration computation for inner water body will not be greatly affected. Considering the effect of a permeable area ratio α, relative location parameter of perforations δ and wave period T, the aforementioned data of 30 experimental scenarios, the dimensional analysis and the least squares method were used to derive an equation of K_2a_2 (K_2a_2=$0.0042\alpha^{0.5}\delta^{0.2}T^{-1}$). It was validated with 6 other experimental scenarios data, which indicates an approximate agreement. Therefore, this equation can be used to compute the DO concentration caused by the water transport through perforated breakwater.

Key words regular wave; perforated breakwater; dissolved oxygen concentration; oxygen transfer coefficient; oxygen transport coefficient

1 Introduction

Breakwaters are widely used for providing protection to ports and water areas for ship mooring (Li *et al.*, 2002; Ozeren *et al.*, 2011; Teh *et al.*, 2012; Suh *et al.*, 2013; Esteban *et al.*, 2014). Due to the mass transport capability loss between inner water and outer water, the conventional breakwater is likely to deteriorate the inner water quality, such as dissolved oxygen (DO) concentration decrease (Daniil *et al.*, 2000). A perforated breakwater is defined as a breakwater that opens perforation(s) in its body. This has the advantages of reducing wave reflection and wave force on structure and improving exchange capacity between inner and outer water, resulting in better inner water quality and improved environmental conditions (Huang *et al.*, 2011; Nikoo *et al.*, 2014).

DO concentration is an important index for measuring water quality and oxygen transfer coefficient is essential to denoting the oxygen transfer capacity. In recent years, many scholars have investigated oxygen transfer coefficient for open channel flow, or regular waves. The oxygen transfer coefficient of open channel flow was expressed in a simple exponential form with average water depth and average velocity (Churchill *et al.*, 1962). Then, water surface slope and wind velocity were introduced into the calculation (Smoot, 1988; Chu and Jirka, 2003). On the other hand, the oxygen transfer coefficient of waves is also influenced by higher wind velocity and it has been found to be proportional to the wind velocity at the standard height of 10m above wave surface (Taylor and Yelland, 2001; Ro and Hunt, 2006). Under lower wind velocity conditions, wave parameters such as wave period, wave height and wave energy have been used in place of wind velocity to externally express the coefficient (Daniil and Gulliver, 1991; Yin *et al.*, 2013).

Generally speaking, inner water DO originates from the atmosphere through the wave surface and from the transport from outer water. The impact of aquatic plant photosynthesis is not considered. The study of DO transport between inner and outer water will improve our understanding of inner water DO concentration change. In this paper, sets of experiments were conducted to measure DO concentration of inner water and outer water with different perforated arrangements and wave parameters. Furthermore, theoretical analysis was used to derive a DO transport coefficient formula between inner water and outer water through perforations. The relationship between oxygen transport coefficient and wave parameters

* Corresponding author. Tel: 0086-532-66781125
E-mail: yinzegao@ouc.edu.cn

was discussed.

2 Experiments

2.1 Experimental Facilities and Setup

In order to investigate DO transport characteristics under regular waves through a perforated breakwater, experiments were conducted in a wave flume at the Hydraulic Laboratory, Ocean University of China. The length, width, and height of the wave flume are 30 m, 0.6 m and 1 m respectively. The regular wave frequencies were controlled at 0.4 s^{-1}, 0.5 s^{-1}, and 0.6 s^{-1} respectively. A vertical perforated breakwater was arranged at the wave flume. The length, width and height of perforated breakwater are 0.02 m, 0.6 m and 0.8 m respectively. Circular holes at two horizontal layers were perforated in the breakwater and their diameters were set to 0.02 m, 0.04 m, and 0.05 m, respectively. The horizontal distance of adjacent holes between edges at the same layer is 0.02 m. The vertical distance of adjacent holes, center to center, at the 2 layers is 0.06 m. Two wave meters were used to measure wave heights and wave lengths of inner water and outer water, respectively. Three DO probes of JPBJ608 type were used to measure the DO concentration after the calibration with Winkler technique (Yakushev *et al.*, 2012). Two DO probes were arranged in inner water and their average value was regarded as the approximate DO concentration of inner water; the other one was arranged in outer water, the measured value being regarded as the DO concentration of outer water. In Fig.1, d is still water depth, d_0 is the circular perforation diameter, d_1 is the distance between the lower edge of lower layer perforations and wave flume bottom, and d_2 is the distance between the lower edge of upper layer perforations and upper edge of lower layer perforations.

2.2 Experimental Procedure

36 experimental scenarios were investigated with different d_0, d_1, d_2, wave generator pedal stroke L_0, wave period T, and initial DO concentration C_0 of inner water (Table 1).

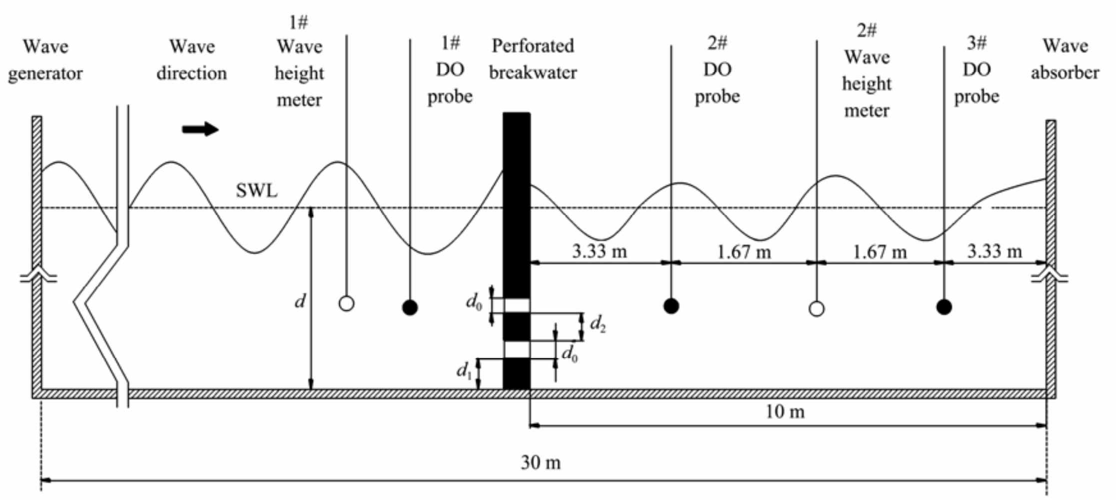

Fig.1 The sketch of experiments.

Table 1 36 scenarios.

Scenarios	d_0 (m)	d_1 (m)	d_2 (m)	L_0 (m)	T (s)	C_0 ($mg\,L^{-1}$)	Scenarios	d_0 (m)	d_1 (m)	d_2 (m)	L_0 (m)	T (s)	C_0 ($mg\,L^{-1}$)
1	0.02	0.10	0.04	0.8	2.00	2.09	19	0.02	0.10	0.04	1.0	2.50	1.86
2	0.02	0.16	0.04	0.8	2.00	1.08	20	0.02	0.16	0.04	1.0	2.50	2.18
3	0.02	0.22	0.04	0.8	2.00	1.98	21	0.02	0.22	0.04	1.0	2.50	2.18
4	0.04	0.10	0.02	0.8	2.00	1.96	22	0.04	0.10	0.02	1.0	2.50	2.1
5	0.04	0.16	0.02	0.8	2.00	1.84	23	0.04	0.16	0.02	1.0	2.50	2.1
6	0.04	0.22	0.02	0.8	2.00	1.87	24	0.04	0.22	0.02	1.0	2.50	2.5
7	0.05	0.10	0.01	0.8	2.00	1.93	25	0.05	0.10	0.01	1.0	2.50	2.2
8	0.05	0.16	0.01	0.8	2.00	1.82	26	0.05	0.16	0.01	1.0	2.50	2.18
9	0.05	0.22	0.01	0.8	2.00	1.99	27	0.05	0.22	0.01	1.0	2.50	1.96
10	0.02	0.10	0.04	1.0	2.00	2.19	28	0.02	0.10	0.04	1.0	1.67	2.33
11	0.02	0.16	0.04	1.0	2.00	1.42	29	0.02	0.16	0.04	1.0	1.67	2.39
12	0.02	0.22	0.04	1.0	2.00	1.47	30	0.02	0.22	0.04	1.0	1.67	2.04
13	0.04	0.10	0.02	1.0	2.00	1.55	31	0.04	0.10	0.02	1.0	1.67	2.02
14	0.04	0.16	0.02	1.0	2.00	1.07	32	0.04	0.16	0.02	1.0	1.67	2.24
15	0.04	0.22	0.02	1.0	2.00	1.45	33	0.04	0.22	0.02	1.0	1.67	2.33
16	0.05	0.10	0.01	1.0	2.00	1.54	34	0.05	0.10	0.01	1.0	1.67	1.25
17	0.05	0.16	0.01	1.0	2.00	1.63	35	0.05	0.16	0.01	1.0	1.67	2.06
18	0.05	0.22	0.01	1.0	2.00	1.71	36	0.05	0.22	0.01	1.0	1.67	1.47

Before the start of an experiment, the perforated breakwater was placed and fixed at the place of 2/3 times the wave flume length from the wave generator side. A piece of thin plastic sheet was placed vertically adjacent to the breakwater in inner water to isolate it from outer water. The wave flume was filled with 0.45 m of fresh tap water. The water temperature was also measured varying from 14.5℃ to 16.8℃. The oxygen scavenger method was used to reduce the DO concentration of inner water. Considering the inner water volume, present DO concentration, the desired DO concentration and the chemical reaction Eq. (1), a suitable amount of Na_2SO_3 was uniformly added into the inner water to lower the DO concentration.

$$2Na_2SO_3 + O_2 \xrightarrow{CoCl_2} 2Na_2SO_4 . \quad (1)$$

$CoCl_2$, at about 0.1% of the weight of Na_2SO_3, was also added to accelerate the reaction speed to ensure that the reaction was finished (Mantha *et al.*, 2001). A mixer was used to mix the inner water to ensure the uniform distribution of DO before the measurement. The thin plastic sheet was taken out slightly to avoid strong turbulence in inner water. The wave pedal was started to generate the desire waves, and the wave height meters and DO probes were started to measure the corresponding data. Everything was recorded every 2 minutes. In the experiments, no breaking wave phenomenon was observed in the inner water body due to the low wave steepness.

3 Analysis of Oxygen Transfer Coefficient and Oxygen Transport Coefficient

3.1 DO Concentration History of Inner Water

The change tendencies of inner water DO concentration were similar to each other within the 36 experimental scenarios. Fig.2 shows the DO history with 2# and 3# DO probes of scenario 30, where t is the time. It was found that DO values of 2# and 3# probes increase faster at first, and then increase slowly after 20 minutes. 50 minutes later, the relative difference between them becomes less than 2.5%, and they approach each other.

Fig.3 shows the results of scenarios of 14, 23, 29, 31, 32, 33 and 35, where C is the measured average DO concentration of inner water. As is shown in Fig.3, C increases rapidly at first, then increases slowly and finally stabilizes. The comparison of scenarios 14, 23 and 32 shows that T plays a significant role in C, and the variation ratio of C increases with a decreasing T. The comparison of scenarios 29, 32 and 35 shows that d_0 is of much importance for C. The comparison of scenarios 31, 32 and 33 shows that d_1 has some influence on C, and the variation ratio of C increases with a decreasing d_1.

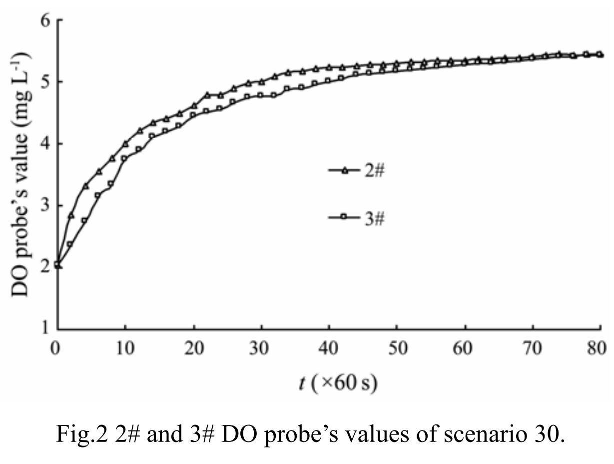

Fig.2 2# and 3# DO probe's values of scenario 30.

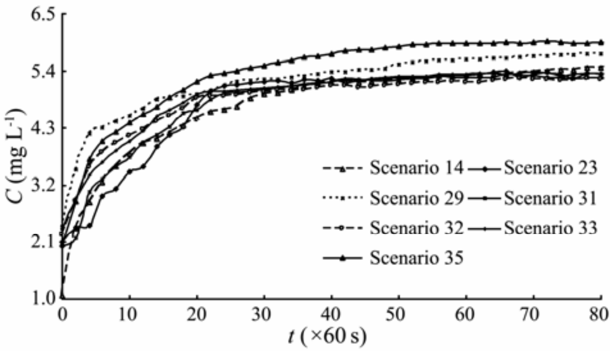

Fig.3 Average DO concentration history of inner water.

3.2 Analysis of Oxygen Transfer Coefficient Through Wave Surface

According to the mass conservation law, the DO variation in inner water over unit time and width, F, consists of 2 parts. One is the amount of oxygen transfer from the atmosphere, F_1, and the other is the amount of DO transport from outer water through perforated holes, F_2. It can be written as follows:

$$F = F_1 + F_2 , \quad (2)$$

$$F_1 = K_1 a_1 (C_S - C) , \quad (3)$$

where $K_1 a_1$ is the oxygen transfer coefficient through wave surface, K_1 is the liquid film mass transfer coefficient through wave surface, C_S is the saturation concentration of DO, and a_1 is the specific surface area of inner water,

$$a_1 = \frac{A_1}{V_1} , \quad (4)$$

where V_1 is the inner water volume per unit width under a wave length scope, A_1 is the wave surface area per unit width under a wave length scope, and it can be written as follows for regular waves,

$$A_1 = 2\int_0^{\frac{L_1}{2}} \sqrt{1 + \frac{\pi^2 H_1^2}{L_1^2} \cos^2\left(\frac{2\pi}{L_1} x\right)} \mathrm{d}x , \quad (5)$$

where L_1 is the wavelength of inner water waves and H_1 is the wave height of inner water. To our knowledge, many scholars paid much attention to the research of K_1, and the following equation was introduced to compute K_1,

$$K_1 = 0.0159 \frac{H_1 \cdot Sc^{-0.5}}{T}, \quad (6)$$

where *Sc* is the Schmidt number.

K_1a_1 of aforementioned scenarios were computed with Eqs. (4)–(6). Fig.4 shows that K_1a_1 from scenarios 19 to 27 were relatively small between $9.2\times10^{-6}\,s^{-1}$ and $2.6\times10^{-5}\,s^{-1}$, K_1a_1 from scenarios 28 to 36 were relatively larger between $5.62\times10^{-5}\,s^{-1}$ and $8.0\times10^{-5}\,s^{-1}$, and K_1a_1 from scenarios 1 to 8 were of medium values between $3.3\times10^{-5}\,s^{-1}$ and $6.0\times10^{-5}\,s^{-1}$.

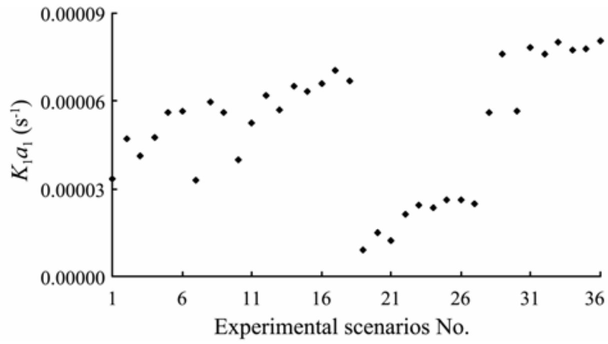

Fig.4 K_1a_1 of 36 experimental scenarios.

3.3 Analysis of Oxygen Transport Coefficient Through Perforations

Similar to Eq. (3), F_2 can be expressed as follows

$$F_2 = K_2a_2(C_S - C), \quad (7)$$

where K_2a_2 is the oxygen transport coefficient through perforations.

The exchange relationship between water and gas could be expressed as follows (Gulliver *et al.*, 1990)

$$\frac{dC}{dt} = \left(K_1a_1 + K_2a_2\right)\left(C_S - C\right). \quad (8)$$

A relative saturation coefficient, *E*, could be obtained by integrating Eq. (8).

$$E = \frac{C - C_0}{C_s - C_0} = 1 - e^{-(K_1a_1 + K_2a_2)t}. \quad (9)$$

Eq.(9) can be rewritten as follows

$$K_2a_2 = -\frac{\ln(1-E)}{t} - K_1a_1. \quad (10)$$

Eq. (10) is used to compute the K_2a_2 variation with time for aforementioned scenarios. It was assumed that K_2a_2 could be regarded as a constant when the relative difference for two adjacent pieces of data was less than 0.2%, and the constants were defined as the stable value of K_2a_2. Fig.5 shows that the stable value of K_2a_2 dispersed from 0.00034 to 0.00085. Fig.4 and Fig.5 show that the stable value of K_2a_2 is 5.7 to 43.9 times of K_1a_1 in general. Therefore the oxygen transport through perforations is the main factor to control the DO concentration increase of inner water.

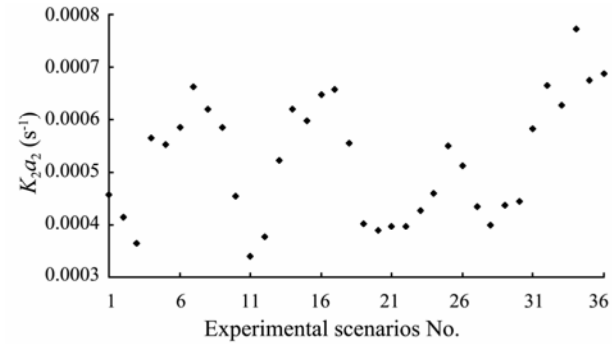

Fig.5 Stable value of K_2a_2 for 36 experimental scenarios.

4 Dimensional Analysis of K_2a_2

Due to the significant contribution of K_2a_2 to DO concentration of inner water, it is imperative to deduce a universal equation for K_2a_2 with the dimensional analysis method.

Due to the small ratio between breakwater length and wave length, the breakwater length effect on K_2a_2 can be ignored in general. The permeable area ratio, α (α is defined as the ratio between all the perforated area and the wave flume cross section area below still water level), the relative location parameter of all the perforations, δ ($\delta = 1 - \frac{\left(d_0 + d_1 + 0.5d_2\right)}{d}$), and wave period, *T*, as the basic variables are selected. K_2a_2 can be expressed as follows

$$K_2a_2 = f\left(\alpha, \delta, T\right). \quad (11)$$

Dimensional harmony theory was used to deduce the following equation,

$$K_2a_2 = \beta\alpha^m\delta^nT^p, \quad (12)$$

where β, *m*, *n* and *p* are undermined coefficients.

The data of 30 aforementioned experimental scenarios are randomly selected and the coefficients β, *m*, *n* and *p* in Eq. (12) are determined with the least square method to be 0.0042, 0.5, 0.2 and −1, respectively. The correlation coefficient is 0.83. So Eq. (12) can be rewritten as follows

$$K_2a_2 = 0.0042\alpha^{0.5}\delta^{0.2}T^{-1}. \quad (13)$$

Eq. (13) shows that *T* is the first factor to influence K_2a_2, α takes the second place and δ has the least influence.

In order to validate the reliability of Eq. (13), the data of the 6 other experiments were used to compare with the results of Eq. (13). Fig.6 shows that the relative error of scenario 2 was 23%, that of scenario 22 was 20%, and the others were all less than 7%. Therefore, the computed K_2a_2 approximately agreed with the experimental data.

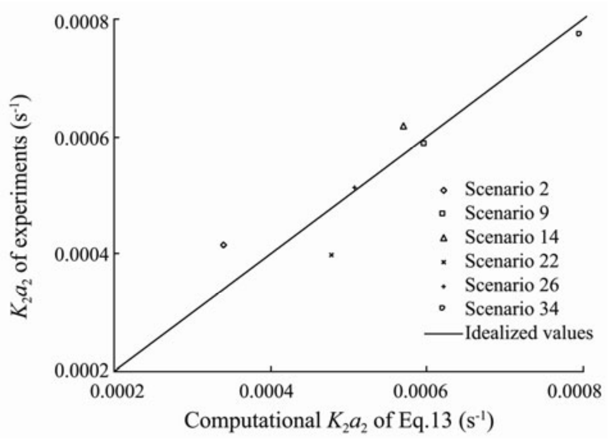

Fig.6 Experimental K_2a_2 and computed values for the 6 other experimental scenarios.

5 Conclusions

36 experimental scenarios were conducted to measure the wave parameters and DO concentration of inner water and outer water for perforated breakwater.

The experimental data were used to compute the oxygen transport coefficient through perforations and the oxygen transfer coefficient through wave surface. It was found that the former is 5.7 to 43.9 times of the latter in general. Therefore the oxygen transport through perforations is the main factor to control the DO concentration increase of inner water body.

The experimental data and the dimensional analysis method were used to derive the equation of oxygen transport coefficient through perforations,

$$K_2a_2=0.0042\alpha^{0.5}\delta^{0.2}T^{-1}.$$

It was validated with other experimental data, and they were approximately in line with each other. Therefore the equation can be used to compute the DO concentration variation caused by water transport through perforated breakwater.

The limitations of this study should be pointed out: Eq. (13) was deduced with 2 layers of perforations, and its applicability needs further validation with more experimental data. The reflection between the wave generator and breakwater affects the wave in front of the breakwater and the dissolved oxygen transport between inner and outer water, which should be considered in future work.

Acknowledgements

The study is funded by the National Natural Science Foundation of China (Nos. 51579229 and 51009123). We would like to thank Y. Li and C. N. Zhang for their support in the experiment.

References

Chu, C. R., and Jirka, G. H., 2003. Wind and stream flow induced reaeration. *Journal of Environmental Engineering*, **129** (12): 1129-1136.

Churchill, M. A., Elmore, H. L., and Buckingham, R. A., 1962. The prediction of stream reaeration rates. *Journal of the Sanitary Engineering Division*, **88** (4): 1-46.

Daniil, E. I., Tsoukala, V. K., and Moutzouris, C. I., 2000. Dissolved oxygen measurements for water quality in a harbour area near Athens, Greece. *Proceedings of the 2000 Joint Conference on Water Resources Engineering and Water Resources Planning and Management*. Minneapolis, Minnesota, 1-8.

Daniil, E. I., and Gulliver, J. S., 1991. Influence of waves on air-water gas transfer. *Journal of Environmental Engineering*, **117** (5): 522-540.

Esteban, M., Jayaratne, R., Mikami, T., Morikubo, I., Shibayama, T., Thao, N. D., Ohira, K., Ohtani, A., Mizuno, Y., Kinoshita, M., and Matsuba, S., 2014. Stability of breakwater armor units against tsunami attacks. *Journal of Waterway, Port, Coastal, and Ocean Engineering*, **140** (2): 188-198.

Gulliver, J. S., Thene, J. R., and Rindels, A. J., 1990. Indexing gas transfer in self-aerated flows. *Journal of Environmental Engineering*, **116** (3): 503-523.

Huang, Z. H., Li, Y. C., and Liu, Y., 2011. Hydraulic performance and wave loadings of perforated/slotted coastal structures: A review. *Ocean Engineering*, **38** (10): 1031-1053.

Li, Y. C., Liu, H. J., Teng, B., and Sun, D. P., 2002. Reflection of oblique incident waves by breakwaters with partially-perforated wall. *China Ocean Engineering*, **16** (3): 329-342.

Mantha, R., Taylor, K., Biswas, N., and Bewtra, J. K., 2001. A continuous system for Fe^0 reduction of nitrobenzene in synthetic wastewater. *Environmental Science and Technology*, **35** (15): 3231-3236.

Nikoo, M. R., Varjavand, I., Kerachian, R., Pirooz, M. D., and Karimi, A., 2014. Multi-objective optimum design of double-layer perforated-wall breakwaters: Application of NSGA-II and bargaining models. *Applied Ocean Research*, **47**: 47-52.

Ozeren, Y., Wren, D. G., Altinakar, M., and Work, P. A., 2011. Experimental investigation of cylindrical floating breakwater performance with various mooring configurations. *Journal of Waterway, Port, Coastal, and Ocean Engineering*, **137** (6): 300-309.

Ro, K. S., and Hunt, P. G., 2006. A new unified equation for wind-driven surficial oxygen transfer into stationary water bodies. *Transactions of the American Society of Agricultural and Biological Engineers*, **49** (5): 1615-1622.

Smoot, J. L., 1988. An examination of stream reaeration coefficients and hydraulic conditions in a pool and riffle stream. PhD thesis. Virginia Polytechnic Institute and State University, Blacksburg.

Suh, K. D., Kim, M., and Kim, S. W., 2013. Comparison of calculation methods of cumulative damage to breakwater armor layer. *Journal of Waterway, Port, Coastal, and Ocean Engineering*, **139** (4): 277-285.

Taylor, P. K., and Yelland, M. J., 2001. The dependence of sea surface roughness on the height and steepness of the waves. *Journal of Physical Oceanography*, **31** (2): 572-590.

The, H. M., Venugopal, V., and Bruce, T., 2012. Hydrodynamic characteristics of a free-surface semicircular breakwater exposed to irregular waves. *Journal of Waterway, Port, Coastal, and Ocean Engineering*, **138** (2): 149-163.

Yakushev, E. V., Vinogradova, E. L., Dubinin, A. V., Kostyleva, A. V., Men'shikova, N. M., and Pakhomova, S. V., 2012. On determination of low oxygen concentrations with Winkler technique. *Oceanology*, **52** (1): 122-129.

Yin, Z. G., David, Z. Z., Liang, B. C., and Wang, L., 2013. Theoretical analysis and experimental study of oxygen transfer under regular and non-breaking waves. *Journal of Hydrodynamics*, **25** (5): 718-724.

(Edited by Xie Jun)